Hindawi
Mathematical Problems in Engineering
Volume 2019, Article ID 2098350, 10 pages
https://doi.org/10.1155/2019/2098350

Research Article

FEM Analysis and Simplified Approach for a Single Energy Pile Subjected to Thermomechanical Loads

Zhong-jin Wang,[1,2,3] **Peng-fei Fang**,[1] **Ri-hong Zhang**,[3] **Kui-hua Wang**,[2] **and Xin-yu Xie**[1,2]

[1]*Ningbo Institute of Technology, Zhejiang University, Ningbo, Zhejiang 315100, China*
[2]*Research Center of Coastal and Urban Geotechnical Engineering, Zhejiang University, Hangzhou 310058, China*
[3]*ZCONE High-tech Pile Industry Holdings Co., Ltd., Ningbo, Zhejiang 315000, China*

Correspondence should be addressed to Peng-fei Fang; fpf@nit.zju.edu.cn

Received 20 November 2018; Revised 15 January 2019; Accepted 22 January 2019; Published 13 February 2019

Academic Editor: Marco Pizzarelli

The distribution of temperature in sand soils was measured through laboratory tests, and the temperature influence on friction resistances at the concrete-soil interface was analyzed. Based on the results of laboratory tests, the finite element model was established using the sequential thermal coupling method. The influences of temperature on the bearing characteristics of energy pile were analyzed. The analysis results show that the cyclic temperature will cause additional displacement along pile depth. It is pointed out that if applied vertical loads at energy pile head exceed the value from which nonlinear settlements would be initiated, irrecoverable additional settlement will occur at pile head. Based on the analysis results, a simplified approach was proposed to estimate the zero point of additional displacement along pile shaft and the additional axial pile force. The comparison between the calculated results obtained by the proposed method and that of ABAQUS on single energy pile was given to verify the accuracy of the proposed method. It is shown that reasonable predictions can be obtained without expensive and time-consuming analyses by the proposed method in this paper.

1. Introduction

Over the past decades, many experimental and theoretical researches have been carried out to analyze the bearing characteristics of pile foundations, because of their extensive application in many infrastructures and structures [1–3]. In recent years, pile foundations have been increasingly used in an innovative form of energy piles, which couples the structural role of pile foundations to that of heat exchangers to exploit the large thermal storage capabilities of the ground, particularly when these energy piles are coupled to heat pumps [4–6]. Due to their economic benefit and environment-friendly advantages, energy piles were widely used around the world recently. Although having been widely used in the world, various aspects of the technology are relatively unknown.

As carrier of heat exchanger, piles will expand and contract while enduring heating and cooling, resulting in thermomechanical phenomena. In the past years, some efforts had been made to study the mechanisms of thermomechanical soil-structure interaction. In situ tests were carried out to investigate the changes of pile characteristics due to temperature, and the results shown that additional thermal stresses would be mobilized in the pile during the heating and cooling. The change of energy pile bearing characteristic was subjected to the restraint conditions of the tested piles, and it was also found that the use of energy piles causes significant thermally induced additional deformation in the pile itself [7–10]. Model tests were also carried out to examine the heat transfer performance and bearing characteristics of piles with embedded tubes under normal working conditions over repeated temperature cycling, and the results show that the thermal stresses were superimposed with the mechanical stresses [11–14]. Centrifuge modeling of soil-structure interaction in energy foundations was also carried out to measure the transient thermomechanical response of

end-bearing energy pile during heating-cooling cycles, and the result shown that the model pile was affected by the heating and cooling cycles [15, 16], being consistent with the conclusion that the effect of temperature on the shear strength of sand, clay, and the clay-concrete interface is negligible [17, 18].

To obtain the characteristics of energy pile foundations during heating-cooling cycles, numerical method was also used to analyze the variations of pile stresses and settlements caused by temperature. Scholars also have carried out many researches to analyze the characteristics of piles during the heating and cooling processes [19–22], and the finite element method was still one of the most extensive methods used to simulate energy piles subjected to a constant mechanical load and a seasonally cyclic thermal load over several years. The results from the above analysis show that the finite element method is a very effective mean to simulate the change of energy pile characteristics.

As discussed above, it is conclude that both the thermal-induced displacements and stresses must be taken into account in the geotechnical design of energy piles despite being acceptable under normal working conditions. The additional axial force and pile shaft friction resistance change are complex, being closely related to the site engineering geological conditions. In this paper, the conduction characteristics of temperature on concrete-soil interface were tested through laboratory tests, and a finite element model was established based on the results from the above laboratory tests. The influences of temperature load on bearing characteristics of a single energy pile were analyzed, and a simplified method was proposed to estimate the zero point of additional displacement and the additional pile axial force was calculated by the proposed method. The comparisons between the calculated results obtained by the proposed method and that of ABAQUS were given to verify the accuracy of the proposed method. It is shown that reasonable predictions can be obtained without expensive and time-consuming analyses by the proposed method in this paper.

2. Laboratory Test

To study the changes of bearing behavior caused by temperature, it is necessary to study the change of temperature with time at the concrete-soil interface and its distribution around the concrete and surrounding soil. A self-developed friction resistance testing device, which can be considering the influence of temperature as shown in Figure 1, was used to measure the temperature conduction and friction change on the concrete-soil interaction surface. The heat pipes were embedded in the prefabricated concrete plate, the distance from the lower surface is 1mm. The temperature sensors were buried in the soil at 1mm from the concrete-soil interface, which is regarded as the pile-soil interface. Test material parameters were shown in Table 1.

The device consists of upper and lower shear boxes with unequal sizes. The upper shear box is fixed on the reaction force rack, and the lower shear box is connected to the reaction force rack through the guide rails, sliding along the guide rails during tests. The upper shear box has a vertical compression plate that can apply normal stress to the soil sample. The loading device is fixed at one side of the lower shear box, and horizontal loads can be applied, and a displacement sensor is provided testing horizontal displacement. The above device was also described by the WANG et al. [13].

Table 1: Parameters of model tests.

Sand parameters	Water content	C_u	C_c	Size (mm)
	5%	3.1	0.9	300x300x75
Concrete parameters				Size (mm)
				500x350x100

The constant temperature heating system is mainly composed of a heating pool, an electric heater, delivery tubes, a thermal fluid, a delivery pump, a temperature probe, and an intelligent thermostat. The temperature probe measures the thermal fluid temperature in the heating pool, and the signal output of the temperature probe is connected with the signal receiving end of the intelligent controller. When the temperature of the thermal fluid in the heating pool reaches the set value, the intelligent temperature controller controls the electric heater to stop working. The delivery pump is connected with the catheter, and the catheter is embedded in the preparation process of the concrete. After the temperature of the thermal fluid reaches a set value, the constant-temperature thermal fluid passes through the inside of the concrete by the delivery tubes. By heat conduction, the temperature of test block can be to a constant value, and the soil is heated through the block. The change of temperature in the soil is measured through the embedded temperature sensor.

11 flexible tubes are embedded in the test concrete block at equal distance, the distance between the hoses and top of the test concrete block is about 10mm, and the length of the hoses is 3 m. When the concrete reaches the certain strength, the wood models were removed and maintained. The surface of the test concrete block is polished, as shown in Figure 2.

When the temperature of heating fluid is stable, the temperature sensor values were begun recording. The tested results were shown in Figure 3. It can be seen that the changes of temperature with time at the concrete soil interface were nonlinear, and the temperature were tending to a constant value after heating for a period of time. From Figure 3, it also could be seen that the frictional resistance with the relative displacement at the concrete-soil interface has no significant changes as the temperature changing. The above results are consistent with existing research conclusions by Yavari et al. [17].

3. Finite Element Analyses for Energy Pile due Temperature

3.1. Finite Element Model. According to the above laboratory test results, it can be seen that the temperature at the concrete-soil interface increases with time, and tends to be constant with time. The temperature has no significant effect on the contact friction between concrete and soils. Based on

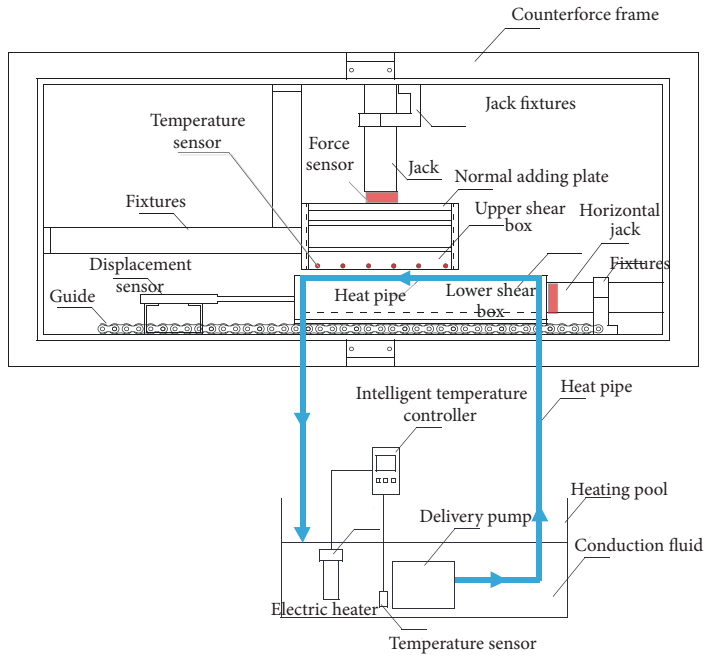

Figure 1: Temperature conduction and friction testing device.

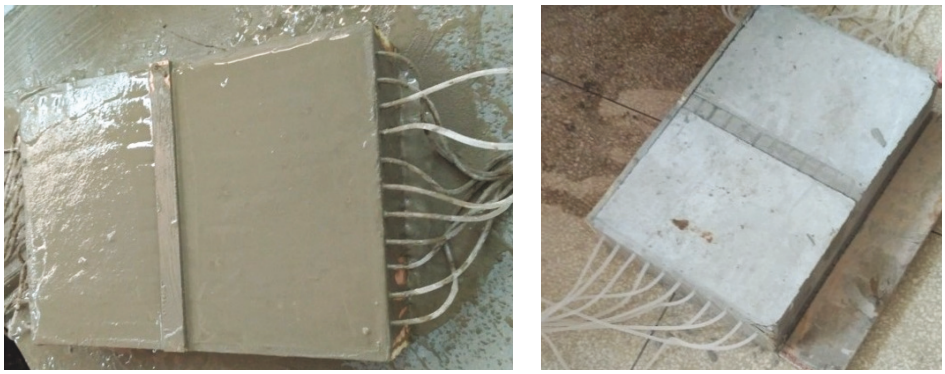

(a) (b)

Figure 2: Molding process of the test concrete block.

the results mentioned above, a finite element model was established, as shown in Figure 4. The length of the pile is 40m, and the diameter of the energy pile is 1000mm. The soil depth is 80m in the direction of the pile depth, and the width value is 40m.

As for the related parameters, Alessandro et al. [6] suggested that the ratio of piles expansion coefficient to that of soils is taken as 0.25~4.0. The values of parameters in the model adopt that recommended by "Thermal design code for civil building" [23] and "Code for Design of Concrete Structures" [24]. The heating surfaces were assumed to be on the spiral-tube surface, ignoring the effects of fluid flow on the change of temperature. The calculation parameters of the model are shown in Table 2.

The axial symmetry finite element model was adopted to analyze the influence of temperature on the pile. The soil adopts More-Coulomb model, and the pile was deemed to be elastic. The effect of the liquid flow on the temperature distribution in the heating pipe was neglected. Based on the measurements in laboratory tests, the influence of temperature change on the mechanical properties of the contact interface was not considered. The finite element analysis adopted sequential thermomechanical coupling method. The implication of this method is that stress does not affect temperature distribution, but temperature causes stress changes. In the process of heat conduction analysis, the heat conduction elements were adopted and the three-dimensional stress elements were adopted in the process of coupled thermomechanical analysis.

According to relevant experimental test data [19, 25] (Li et al., 2013), after the energy pile was heated for a certain period of time, the overall temperature of the pile is increased by

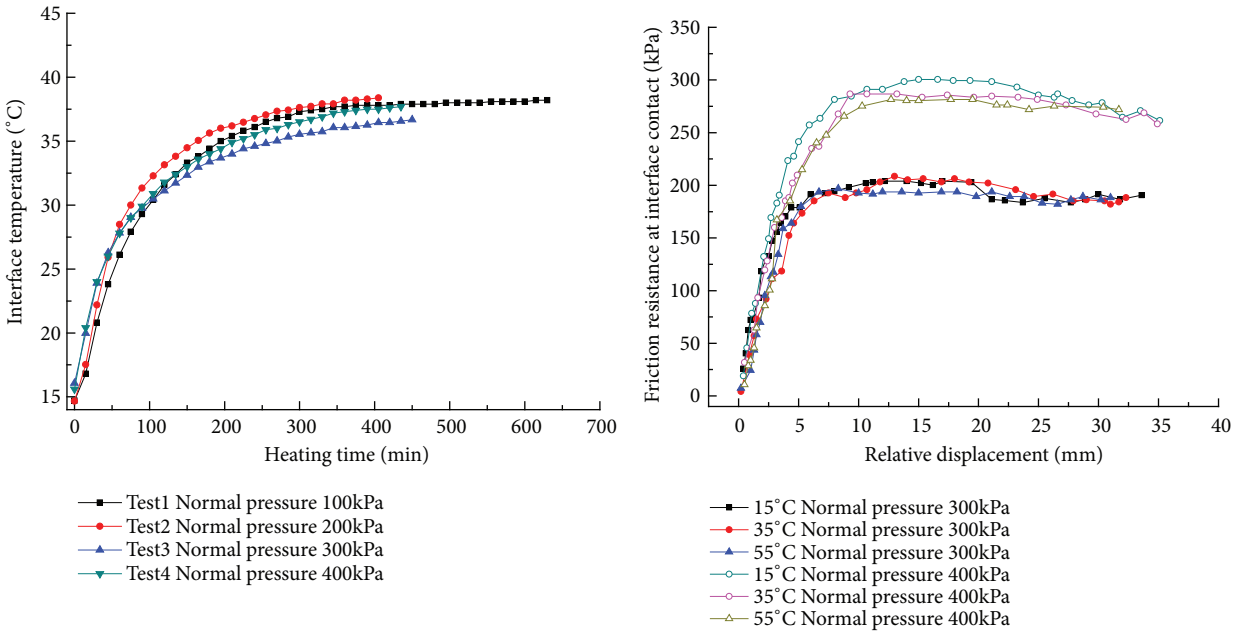

(a) Temperature changes at pile-soil interface with time

(b) Curves of interface friction resistance-displacement

Figure 3: Experimented results of temperature conduction and friction.

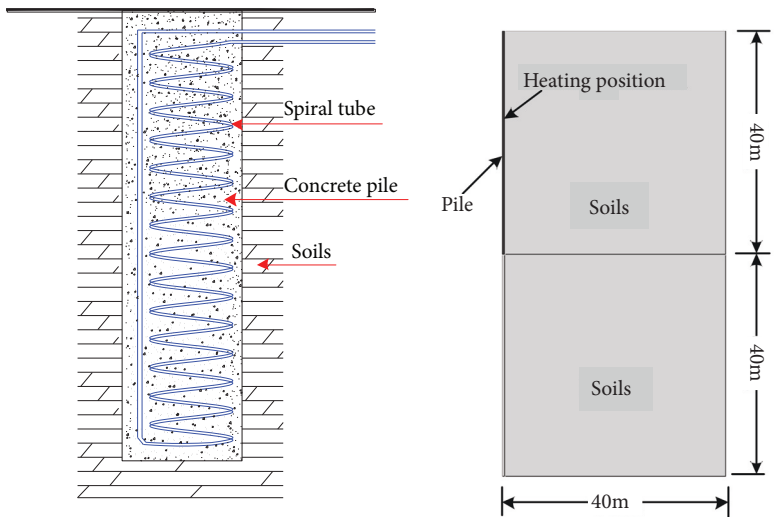

(a) (b)

Figure 4: The simplified diagram for calculation model.

Table 2: Parameters of finite element model.

Parameter	Value	Parameter	Value
Elastic modulus of pile GPa	30	Pile unit weight kN/m^3	25
Soil elastic modulus MPa	20	Soil unit weight kN/m^3	20
Coefficient of linear thermal expansion for pile °C^{-1}	1x10^{-5}	Friction angle of soil °	30
Coefficient of linear thermal expansion for soil °C^{-1}	2x10^{-6}	Soil Poisson's ratio	0.35
Pile conductivity W/m/K	1.74	Soil cohesion kPa	5
Specific heat capacity of soil J/kg/K	1305	Pile Poisson's ratio	0.15
Specific heat capacity of pile J/kg/K	1706	Soil conductivity W/m/K	1.16

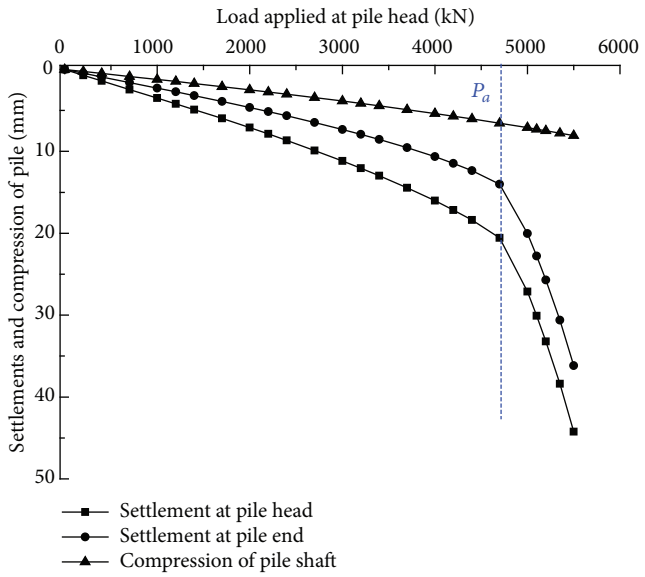

Figure 5: Curves of load and displacements of pile.

about 20°C, and the measured soil temperature at a certain depth was 17.5-22.5°C below the ground (Li et al., 2013) [26]. The initial temperature of the adopted model above was regarded as 20°C. After heating, the increase of temperature was set to be 20°. The temperature load was applied according to the actual increase from the laboratory test as shown in Figure 2(a). The finite element model adopted the sequential thermocoupling analysis method. In the thermal analysis process, the heat transfer element was adopted and three-dimensional stress element is used in the coupling analysis process. The bottom and the sides of the model were fixed, and the top is unconstrained.

3.2. Analysis Results. The load-settlement curves from the calculated model were shown in Figure 5, and it could be seen that while pile top load exceeded 4700kN, the settlement began to drop steeply. The influences of temperature on pile top displacements and pile end settlements of energy piles were shown in Figure 6. From Figure 6, it could be seen that the additional displacements and end settlements caused by temperature have no significant difference when the pile top has no load and the applied load was equal to 1000kN and 3000kN. While the pile top load increases more than about 4700kN, the pile top displacements and end settlements caused by cycle heating and cooling were becoming obvious. As the pile top load increases, the pile top displacements caused by heating were decreased, but the pile end settlements become lager. With the progress of cooling, the additional pile top settlements caused by heating increased with increase of the pile top load. Through the above analyses, it could be concluded that the level of pile top load has significant influence on the displacements and end settlements caused by temperature. The displacements along the pile depth caused by cycle heating and cooling were shown in Figure 6. From Figure 6, it could be seen that the displacements along pile depth changed linearly. The lines for changes of temperature-induced displacements along pile depth were parallel, and the temperature-induced displacements along pile depth increase as the pile top loads increasing.

It could be seen from Figure 8 that the loads at pile top had great influences on changes of pile axial forces due to temperature. The pile top load increases to the value, P_a, from which the applied pile heat load could lead to pile end settlement suddenly increasing, the relative displacement of the pile and surrounding soils increasing, the side friction resistance fully developing, and the axial force caused by temperature significantly being reduced. As the pile top loads increasing, the maximum change of pile axial force caused by the temperature reduced. While the load at pile top is less than P_a, the maximum change of pile axial force caused by heating is approximately 25m below pile top. When the loads at the top of the pile were larger than the value of P_a, the maximum changes of energy pile axial force due to heating were reduced with increase of pile top loads and the corresponding positions of the maximum changes of axial force rise up along the pile depth with increase of pile top load.

The displacement differences between pile top and end caused by temperature were shown in Figure 9. It can be seen from Figure 9 that the displacement differences of energy pile caused by heating and cooling were approximately consistent at different load levels.

As discussed above, the conclusion that heating and cooling would lead to additional displacement of energy pile with pile head load of P_a from which nonlinear settlements begun to occur and from safety view of engineering, loads applied at energy pile top should not be heavier than the value of P_a. Within the load value of P_a mentioned above, the displacement of energy pile caused by heating could be eliminating with the process of cooling, as shown in Figure 9.

4. Simplified Calculation Method

4.1. Analysis of Pile under Thermomechanical Load. Even though many existing methods about the settlement of pile foundation and load transfer mechanism analysis of single pile, these methods for the energy pile are not very applicable due to the temperature load.

The behavior between the pile shaft and the surrounding soils in this paper is described by a simple linear model. For the linear relationship, the pile side friction is increasing linearly with gradually increasing relative displacement between pile shaft and surrounding soils. The relationship between the pile end loads and the settlements also can be expressed by the linear model based on the existing research results. The relationships can be expressed in the following:

$$\tau_z = k_s \Delta s_z$$
$$\tau_b = k_b s_b \quad (1)$$

where $\tau(z)$ is the shaft shear stress at a given depth z, k_s is the initial stiffness of the soil surrounding pile shaft, Δs_z is the pile-soil relative displacement developed in the pile-soil interface at a given depth z. τ_b is the pile end resistance, k_b is initial soil stiffness at the pile base, and s_b is the pile end

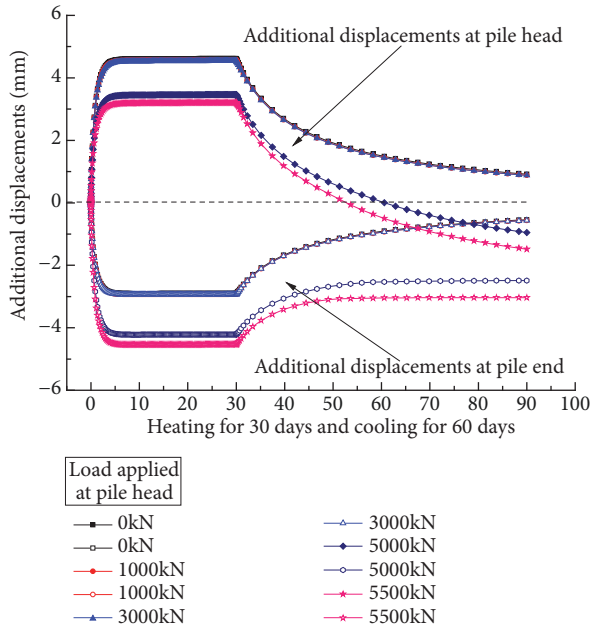

Figure 6: Displacements of pile top and end caused by temperature.

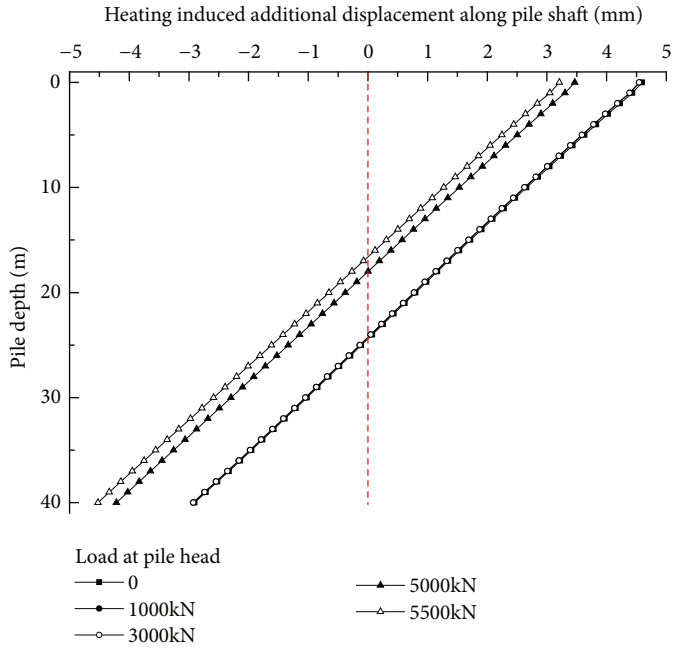

Figure 7: Temperature-induced displacements along pile depth.

settlements. The coefficients k_s and k_b can be obtained by the proposed method in the references [1–3, 27].

As discussed above, it can be seen that there was a zero point of displacement change at which the additional displacement caused by temperature was zero, while the pile top load was not heavier than the value, P_a, that leading to nonlinear settlement of pile top, as shown in Figures 6 and 7. Position of the point can be obtained by the condition of mechanical equilibrium due to heating, as shown in Figure 10. Assuming that the temperature caused expansions of soil surrounding pile end and pile shaft were negligible, only the expansion of the pile is considered. The behavior between the pile shaft and the surrounding soils and the relationship between pile end load and settlement were all expressed by linear models.

The zero point of displacement change is considered as origin of coordinate, and the length from zero point to the pile head has the value of l_1. l_1 can be written by the equilibrium expression:

$$\int_0^{l_1} 2\pi r_0 k_s \lambda_p \Delta T l dl = \int_0^{L-l_1} 2\pi r_0 k_s \lambda_p \Delta T l dl + \pi r_0^2 k_b \lambda_p \Delta T \left(L - l_1\right) \tag{2}$$

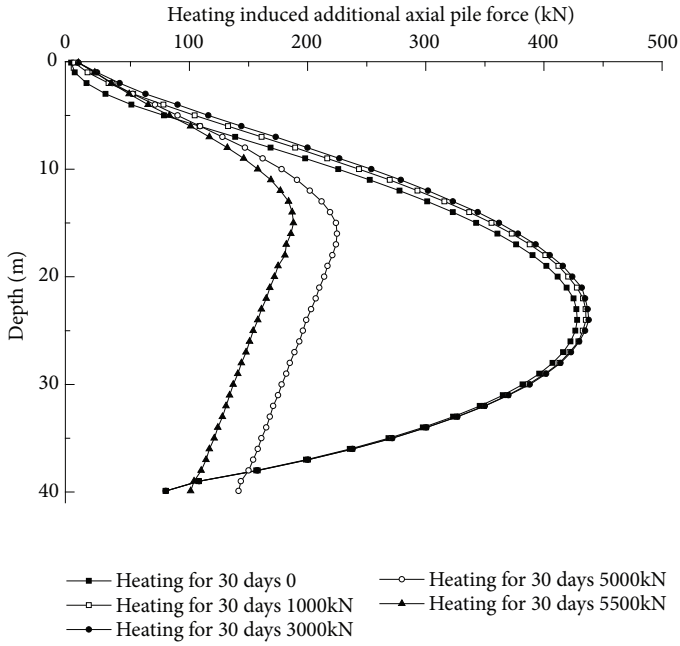

Figure 8: Variations of pile axial force caused by temperature.

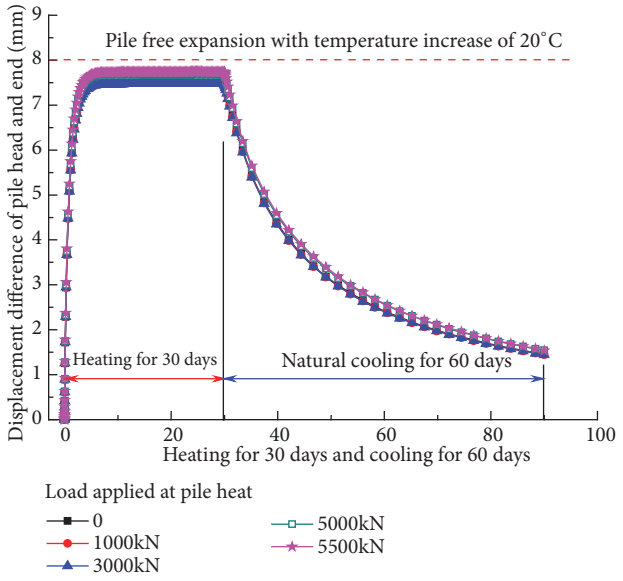

Figure 9: Settlement difference caused by heating 30d and cooling 60d.

where λ_p is the coefficient of linear expansion for pile and ΔT is the temperature increase of pile body. Thus, the zero point of displacement change l_1 can be obtained in

$$l_1 = \frac{k_s L^2 + r_0 k_b L}{2k_s L + r_0 k_b} \tag{3}$$

The additional axial pile shaft force from the pile head to the zero point can be obtained by

$$\Delta p_z = \int_0^z 2\pi r_0 k_{s1} \Delta T \lambda_p (l_1 - l)\, dl \tag{4}$$

The analytic solutions to (4) can be expressed in

$$\Delta p_z = 2\pi r_0 k_{s1} \Delta T \lambda_p l_1 z - \pi r_0 k_{s1} \Delta T \lambda_p z^2 \tag{5}$$

The additional axial pile shaft force from the zero point to the pile end can be obtained by

$$\Delta p_z = \pi r_o^2 k_b \Delta T l_2 \lambda_p + \int_{l_1}^z 2\pi r_0 k_s \Delta T \lambda_p (L - z)\, dz \tag{6}$$

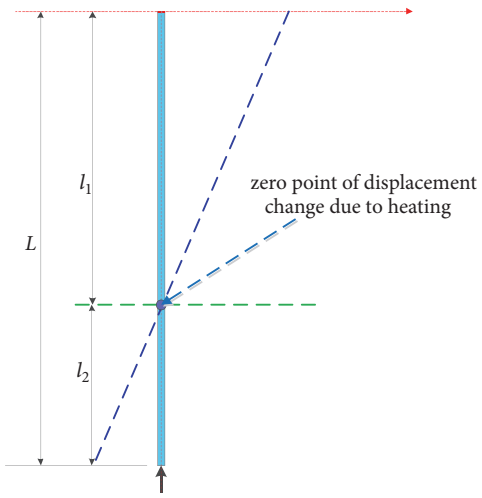

Figure 10: Zero point of displacement change.

The analytic solutions to (6) can be expressed in

$$\Delta p_z = \pi r_o^2 k_b \Delta T l_2 \lambda_p + 2\pi r_0 k_s \Delta T \lambda_p L (z - l_1) - \pi r_0 k_s \Delta T \lambda_p \left(z^2 - l_1^2\right) \quad (7)$$

In multilayered soils, assume the zero point of displacement change is in the *ith* layer and the length from the *ith* layer soil heat to the zero point is l_1, as shown in Figure 11. The zero point of displacement change can be obtained by

$$\sum_{j=0}^{i-1} \int_{l_j}^{l_{j+1}} 2\pi r_0 k_{sj} \lambda_p \Delta T l dl + \int_0^{l_1} 2\pi r_0 k_{si} \lambda_p \Delta T l dl = \sum_{j=i+1}^{n} \int_{l_j}^{l_{j+1}} 2\pi r_0 k_{sj} \lambda_p \Delta T l dl + \int_0^{L_i - l_1} 2\pi r_0 k_{si} \lambda_p \Delta T l dl + \pi r_0^2 \left(L - l_1 - \sum_{j=1}^{i-1} L_j\right) \Delta T \lambda_p k_b \quad (8)$$

All the parameters in the above equation are shown in Figure 11. The additional axial pile shaft force from the pile head to the zero point can be obtained by the following, assuming that the relative displacements between the pile shaft and the surrounding soils are in linear relationship in all the multilayered soils:

$$\Delta p_z = \sum_{j=0}^{i-1} \int_{\sum_{m=0}^{j} l_m}^{\sum_{m=0}^{j+1} l_m} 2\pi r_0 k_{sj} \lambda_p \Delta T \left(\sum_{j=0}^{I-1} L_i + l_1 - z\right) dz + \int_{\sum_{m=0}^{i-1} l_m}^{z} 2\pi r_0 k_{si} \lambda_p \Delta T \left(\sum_{j=0}^{I-1} L_i + l_1 - z\right) dz \quad (9)$$

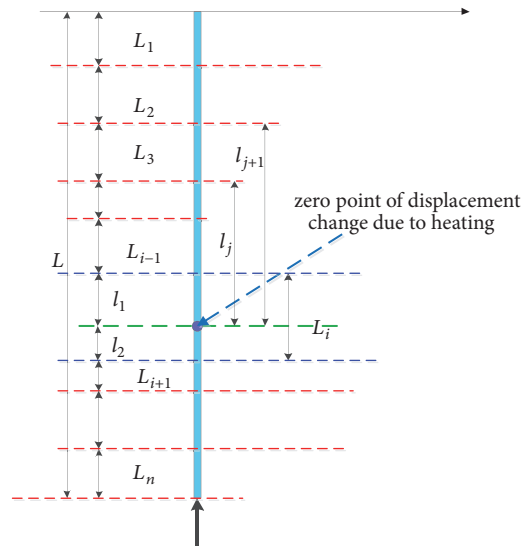

Figure 11: Calculation model for zero point in multilayered soils.

The additional axial pile shaft force from the pile top to the zero point can be obtained by

$$\Delta p_z = \pi r_o^2 k_b \Delta T \left(L - \sum_{j=0}^{I-1} L_j - l_1\right) \lambda_p + \sum_{j=1}^{i} \int_{\sum_{m=I}^{j} l_m}^{\sum_{m=I}^{j+1} l_m} 2\pi r_0 k_{sj} \lambda_p \Delta T \left(\sum_{j=I}^{n-I} L_j - l_1 - z\right) dz + \int_{\sum_{m=I}^{n-i+1} l_m}^{z} 2\pi r_0 k_{si} \lambda_p \Delta T \left(\sum_{j=I}^{n-i+1} L_i - l_1 - z\right) dz \quad (10)$$

In order to determine the specific position of layers in (10), the procedure can be adopted to calculate

(1) Confirm the values of k_{si} in the *ith* soil layer.

(2) Assume that the zero point is in the lowest layer and calculate to obtain the value of l_1, as shown in Figure 11.

(3) If the solution of l_1 is negative, then assuming the zero point is in the *(n-1)th* as shown in Figure 11. Continue to calculate the solution to (8) until obtaining the positive value of l_1.

(4) Calculate the additional axial pile shaft force using (9) and (10) along pile shaft.

5. Case Study

The proposed method is an approximate calculation method, and the existing tests mainly focused on heat transfer analysis of pile to study the responses of heat conduction, and the bearing characteristics of field tested pile were also carried out by many scholars. But the bearing characteristics were influenced by many factors such as the stratums and groundwater flow. Therefore, the finite element method is adopted to compare with the results obtained by the above proposed method. The parameters in the analysis adopted the values from the Table 3.

Comparisons between the results form ABAQUS and those computed by the proposed approach are shown in

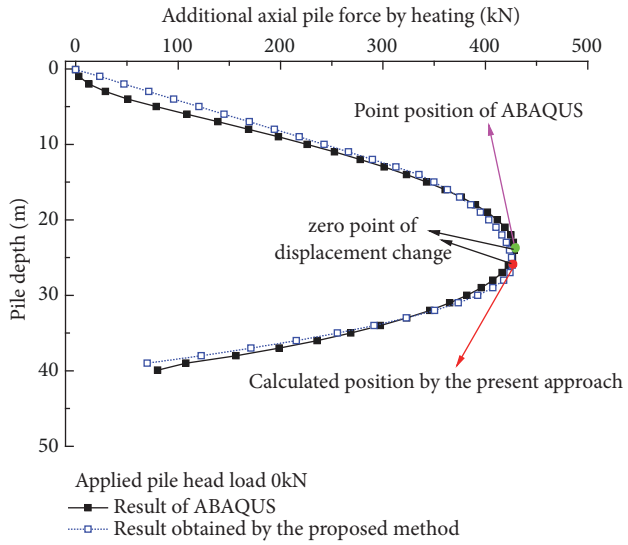

Figure 12: Result comparisons between the proposed method and finite method (ABAQUS).

Table 3: Parameters of case study.

Layer of soils	Thickness of soil layer (m)	Parameters	Values(kPa/mm)
Layer 1	5	k_{s1}	1.094
Layer 2	5	k_{s1}	1.276
Layer 3	5	k_{s1}	2.161
Layer 4	5	k_{s1}	2.719
Layer 5	5	k_{s1}	2.771
Layer 6	5	k_{s1}	2.875
Layer 7	5	k_{s1}	3.066
Layer 8	5	k_{s1}	3.241
l_1=26.31 m (Obtained by the proposed method)			
l_1 = 24.65 m (Obtained by ABAQUS)			
r_{pile}=0.5m, H_{pile}=40m, λ_{pile} $^{\circ}C^{-1}$=1x10^{-5}, k_{b1}=28.91kPa/mm			

Figure 12. Comparison between the curves computed by the proposed approach and that of ABAUQS is shown in Figure 12. Figure 12 shows that the additional displacements along pile shaft caused by heating calculated by the proposed method are generally consistent with the finite method results.

6. Conclusions

As discussed above, the following conclusions can be obtained:

(1) The frictional resistance at the concrete-soil interface has no obvious relationship to the variation of temperature. The cycle temperature would lead to unrecoverable additional displacement at energy pile heat with heavy loads from which nonlinear settlement occurred on the load-settlement curve.

(2) The position of the zero point of displacement change has no obvious relationship to temperature change of pile body. The main factors of influence on the point are the initial soil stiffness at the pile base and shear stiffness of soils surrounding pile and the coefficients of linear expansion for pile.

(3) The proposed method can be used to estimate the zero point of additional displacement and additional pile axial force along pile length.

Data Availability

All the data used to support the findings of this study are included within the article.

Conflicts of Interest

The authors declare that there are no conflicts of interest regarding the publication of this paper.

Acknowledgments

This research presented in this paper was supported by the National Natural Science Foundation of China (Research Grant nos. 51708496 and 51579217) and the Zhejiang Provincial Natural Science Foundation (Research Grant nos. LY16E080010, LY19E080013, and Q19E080021). These financial supports are gratefully acknowledged.

References

[1] Z. Wang, X. Xie, and J. Wang, "A new nonlinear method for vertical settlement prediction of a single pile and pile groups in layered soils," *Computers & Geosciences*, vol. 45, pp. 118–126, 2012.

[2] Q.-Q. Zhang, R.-F. Feng, S.-W. Liu, and X.-M. Li, "Estimation of uplift capacity of a single pile embedded in sand considering arching effect," *International Journal of Geomechanics*, vol. 18, no. 9, Article ID 06018021, 2018.

[3] Q. Zhang, S. Liu, R. Feng et al., "Analytical method for prediction of progressive deformation mechanism of existing piles due to excavation beneath a pile-supported building," *International Journal of Civil Engineering*, 2018.

[4] H. Brandl, "Energy foundations and other thermo-active ground structures," *Géotechnique*, vol. 56, no. 2, pp. 81–122, 2006.

[5] L. Laloui and A. Di Donna, *Energy Geostructures: Innovation in Underground Engineering*, Wiley-ISTE, 2013.

[6] F. Alessandro, L. Rotta, and L. Laloui, "The interaction factor method for energy pile groups," *Computers & Geosciences*, vol. 80, pp. 121–137, 2016.

[7] B. L. Amatya, K. Soga, P. J. Bourne-Webb, T. Amis, and L. Laloui, "Thermo-mechanical behaviour of energy piles," *Géotechnique*, vol. 62, no. 6, pp. 503–519, 2012.

[8] P. Hemmingway and M. Long, "Energy piles: Site investigation and analysis," *Proceedings of the Institution of Civil Engineers: Geotechnical Engineering*, vol. 166, no. 6, pp. 561–575, 2013.

[9] K. D. Murphy, J. S. McCartney, and K. S. Henry, "Thermo-mechanical characterization of a full-scale energy foundation," *From Soil Behaviour Fundamentals to Innovations in Geotechnical Engineering*, vol. 233, pp. 617–628, 2014.

[10] R. Saggu and T. Chakraborty, "Cyclic thermo-mechanical analysis of energy piles in sand," *Geotechnical and Geological Engineering*, vol. 33, no. 2, pp. 321–342, 2015.

[11] N. Yavari, A. M. Tang, J. Pereira, and G. Hassen, "A simple method for numerical modelling of mechanical behaviour of an energy pile," *Géotechnique Letters*, vol. 4, no. 2, pp. 119–124, 2014.

[12] C.-L. Wang, C. W. W. Ng, H.-L. Liu, D. Wu, and G.-Q. Kong, "Model tests of energy piles with and without a vertical load," *Environmental Geotechnics*, vol. 3, no. 4, pp. 203–213, 2016.

[13] W. Zhong-jin, Z. Ri-hong, and W. Kui-hua, "Bearing characteristic of static drill rooted pile considering condition of energy carrier," *Journal of Zhejiang University (Engineering Science)*, vol. 53, no. 1, pp. 11–18, 2019 (Chinese).

[14] G. Kong, D. Wu, H. Liu, L. Laloui, X. Cheng, and X. Zhu, "Performance of a geothermal energy deicing system for bridge deck using a pile heat exchanger," *International Journal of Energy Research*, vol. 43, no. 1, pp. 596–603, 2019.

[15] M. A. Stewart and J. S. McCartney, "Centrifuge modeling of soil-structure interaction in energy foundations," *Journal of Geotechnical and Geoenvironmental Engineering*, vol. 140, no. 4, Article ID 04013044, 2014.

[16] C. W. W. Ng, C. Shi, A. Gunawan, L. Laloui, and H. L. Liu, "Centrifuge modelling of heating effects on energy pile performance in saturated sand," *Canadian Geotechnical Journal*, vol. 52, no. 8, pp. 1–13, 2015.

[17] N. Yavari, A. M. Tang, J.-M. Pereira, and G. Hassen, "Effect of temperature on the shear strength of soils and the soil–structure interface," *Canadian Geotechnical Journal*, vol. 53, no. 7, pp. 1186–1194, 2016.

[18] V. T. Nguyen, A. M. Tang, and J.-M. Pereira, "Long-term thermo-mechanical behavior of energy pile in dry sand," *Acta Geotechnica*, vol. 12, no. 4, pp. 729–737, 2017.

[19] L. Laloui, M. Nuth, and L. Vulliet, "Experimental and numerical investigations of the behaviour of a heat exchanger pile," *International Journal for Numerical and Analytical Methods in Geomechanics*, vol. 8, no. 30, pp. 763–781, 2006.

[20] W. Zhang, H. Yang, L. Fang, P. Cui, and Z. Fang, "Study on heat transfer of pile foundation ground heat exchanger with three-dimensional groundwater seepage," *International Journal of Heat and Mass Transfer*, vol. 105, pp. 58–66, 2017.

[21] Y. Zhang, T.-F. Yin, G.-F. Fan et al., "Study on bearing capacity of pile foundation considering the heat exchange effect," *Journal of Water Resources and Architectural Engineering*, vol. 15, no. 03, pp. 203–208, 2017.

[22] A. Zarrella, G. Emmi, R. Zecchin, M. De Carli et al., "An appropriate use of the thermal response test for the design of energy foundation piles with U-tube circuits," *Energy and Buildings*, vol. 134, pp. 259–270, 2017.

[23] "GB 50176-93 Thermal design code for civil building" (Chinese), 1993.

[24] "GB 50010-2010 Code for design of concrete structures" (Chinese), 2010.

[25] W. H. Thompson III, *Numerical Analysis of Thermal Behavior and Fluid Flow in Geothermal Energy Piles*, Virginia Polytechnic Institute and State University, Blacksburg, Va, USA, 2013.

[26] S.-Q. Gui and X.-H. Cheng, "In-situ tests on structural responses of energy piles during heat exchanging process," *Chinese Journal of Geotechnical Engineering*, vol. 36, no. 6, pp. 1087–1094, 2014 (Chinese).

[27] M. F. Randolph and C. P. Wroth, "An analysis of the vertical deformation of pile groups," *Geotechnique*, vol. 29, no. 4, pp. 423–439, 1979.